Molecular Dynamics Simulations Reveal Inhomogeneity-Enhanced Stacking of Violanthrone-78-Based Polyaromatic Compounds in n -Heptane–Toluene Mixtures

ARTICLE *in* THE JOURNAL OF PHYSICAL CHEMISTRY B · JUNE 2015

Impact Factor: 3.3 · DOI: 10.1021/acs.jpcb.5b04481 · Source: PubMed

2 AUTHORS:

Cuiying Jian

University of Alberta

5 PUBLICATIONS **24** CITATIONS

SEE PROFILE

Tian Tang

University of Alberta

62 PUBLICATIONS **776** CITATIONS

SEE PROFILE

THE JOURNAL OF PHYSICAL CHEMISTRY B

Article

pubs.acs.org/JPCB

Molecular Dynamics Simulations Reveal Inhomogeneity-Enhanced Stacking of Violanthrone-78-Based Polyaromatic Compounds in *n*-Heptane−Toluene Mixtures

Cuiying Jian and Tian Tang*

Department of Mechanical Engineering, University of Alberta, Edmonton, AB T6G 2G8, Canada

Supporting Information

ABSTRACT: We elucidated the effect of inhomogeneity in solutes on the aggregation of our representative polyaromatic (PA) compounds through a series of molecular dynamics simulations. Two kinds of solutes, a single type of PA compounds and a mixture of four types of PA compounds, were simulated in toluene, *n*-heptane, and heptol (mixture of toluene and *n*-heptane). The geometries of the resultant aggregates were quantified using gyradius ratios. Our results revealed that in toluene, while a single type of PA compound can only form short-cylinder-like aggregates, by having a solute mixture, parallel stacking of PA cores is enhanced, leading to the formation of one-dimensional (1D) rod-like structure. The enhanced stacking is caused by collective arrangement of the PA molecules; i.e., PA compounds of different types appear in an alternating manner in the aggregate. In addition, while the aggregated geometries of a single type of PA compounds were found to be affected by the composition of the solvents, the existence of the 1D structure formed by mixture seems to be insensitive to the solvents. On the other hand, the longest range of stacking is achieved by having a small amount of toluene ("good" solvent) in *n*-heptane ("bad" solvent).

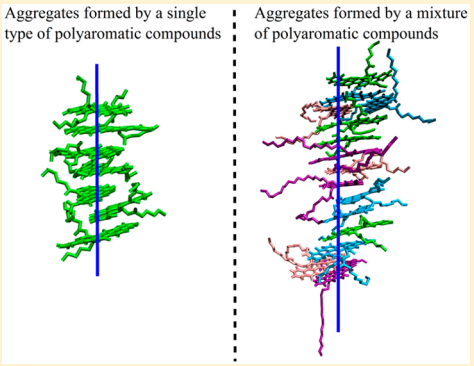

1. INTRODUCTION

The aggregation of polyaromatic (PA) compounds has gained an increasing interest, mainly due to their promising applications in the design of optical and electronic devices[1] as well as their serious effects in processing industrial materials.[2] For instance, one-dimensional (1D) nanostructures, self-assembled via parallel stacking ($\pi-\pi$ stacking) of PA molecules, are finding their applications in organic photovoltaics, sensors, nanophotonics, and nanoelectronics.[3] On the other hand, the highly stable aggregates formed by industrial PA compounds, such as asphaltenes, have caused many problems in heavy oil processing associated with well production and exploration, pipeline transport, oil refining, and emulsion stabilization.[4−6]

Many factors can influence the aggregated structures of PA compounds, such as their molecular structures,[7−10] type of solvents,[11] solution concentrations,[12,13] and external conditions including temperature as well as pressure.[10,14,15] Among these factors, the effect of solvents and solute molecular structures has been extensively investigated for different types of PA compounds, such as the derivatives of perylenetetracarboxylic diimide (PTCDI),[16] hexabenzocoronene (HBC),[16] pyrene,[17] and violanthrone.[18−21] For instance, a series of studies by Zang et al.[1,22−25] have revealed the vital role played by solvents and the side-chain substituents of PTCDIs. It was found PTCDI molecules modified with acid groups could self-assemble into 1D nanostructure in aqueous solvent upon the adjustments of solution pH,[24] whereas in organic solvents, 1D nanostructures could be generated from PTCDIs substituted with alkyl and alkyloxy side chains.[22,23,25] In addition, under the same conditions in organic solvents while PTCDIs modified with linear alkyl chains could form well-defined 1D nanobelt structures, PTCDI molecules modified with nonyldecyl groups could only generate irregular chunky aggregates.[21,22] For violanthrone derivatives, our previous work explored the effect of solvents on the geometry of the aggregates.[19−21] Given a particular type of PA molecules, results from molecular dynamics (MD) simulations revealed[19−21] aggregates of distinct geometry characteristics in different solvents: while most PA cores were simply entangled together in water, leading to sphere-like aggregates,[19] the aggregated PA cores in *n*-hetpane resembled 1D rod-like geometry, self-assembled mainly via $\pi-\pi$ stacking.[21] In toluene, although $\pi-\pi$ stacking of PA cores was still widely observed, the range of the stacking was much smaller compared with that in *n*-hetpane, and hence a 1D geometry was absent.[20]

These previous studies mainly focused on the aggregated structures formed by a single type of PA compounds. However, impurity (inhomogeneity) in solute can exist in practical applications. For instance, asphaltenes are a mixture of different types of PA molecules.[26,27] Therefore, it is of interest to study the aggregation behavior of mixed PA compounds. In fact, some recent studies have reported interesting findings on the

Received: May 10, 2015
Revised: June 15, 2015
Published: June 16, 2015

DOI: 10.1021/acs.jpcb.5b04481
J. Phys. Chem. B 2015, 119, 8660−8668

aggregation of a mixture of molecules possessing aromatic features. Shown by Ryan et al.,[28] equimolar mixtures of Fmoc-Phe and Fmoc-F5-Phe readily coassembled to form two-component fibrils and hydrogels under conditions where Fmoc-Phe alone failed to self-assemble. Demonstrated by Shakai et al.,[29] mixing multiple types of amyloid peptides provides remarkable control over the self-assembled structures, which is very difficult to achieve by a single type of peptide. Recently, to enhance the photoconductivity of 1D nanostructure formed by PTCDIs, Hayward et al.[30,31] reported the coupled aggregation of poly(3-hexylthiophene) (P3HT, polymerized thiophene) and dioctyl-substituted PTCDI in organic solvent 1,2-dichlorobenzene. It was found that the aggregates resembled "shish-kebab" type of structures consisting of central PTCDI 1D nanowires flanked by P3HT fibrils, where these fibrils were proposed to reduce the lateral association of PTCDI molecules.[30,31]

Despite these interesting works, theoretical study on the aggregation of PA compounds has been quite limited. To mimic industrial asphaltenes, Kuznicki et al.[17] simulated the aggregation of mixed PA compounds in water, toluene, and heptane. The two types of PA compounds in their study have distinct structures: one possessing a single core with side-chain substituents and the other consisting of two small aromatic regions interconnected by aliphatic chains. The dominant structural feature of the aggregates was found to be the stacking of the polyaromatic rings, which could occur between the molecules of the same type or between molecules of different structures. In the work of Zhang et al.,[32] dissipative particle dynamics simulations were performed on model heavy crude oil systems. It was found that small PA compounds (with two hexa-particle rings), used to represent resins, did not participate in forming aggregates with large PA molecules (with at least three hexa-particle rings) which represented asphaltenes. While these two studies and a few other works[33−38] have probed the aggregation phenomena of their given mixtures, how mixing molecules of different structures may affect the overall aggregated morphologies was not investigated. In addition, no direct comparison was made between mixture and a pure type of PA compounds. Will different PA molecules in the mixture demonstrate any collective behaviors? And if so, will such behaviors depend on the property of solvent? To answer these questions, in the present work, we performed MD simulations on the aggregation of two kinds of solutes: one involving a single type of PA molecule and the other containing a mixture of four types of systematically varied PA molecules. Comparison between these two kinds of solutes provides direct information on the contribution of inhomogeneity to aggregation. Furthermore, these two kinds of solutes were solvated in several different organic solvents, which allows us to explore the role of solvents. The remainder of the paper is organized as follows: the molecular models, systems simulated, and computational methods are introduced in section 2; section 3 presents a detailed examination on the aggregates of the two kinds of solutes in different solvents; and final conclusions are given in section 4.

2. METHODS

Four PA compounds (developed based on Violanthroe-78 and named VO-4C, VO-8C, VO-12C, and VO-16C), with different aromatic/aliphatic ratios, were used in this work, and their chemical structures are shown in Figure 1. As can be seen, these four PA compounds all consist of a fused PA core with peripheral side chains, similar to the island molecular model[2] proposed for asphaltenes in petroleum industry as well as many organic compounds used in optoelectronics devices.[1] The detailed design and construction schemes of these molecular models are available from our previous studies.[19−21]

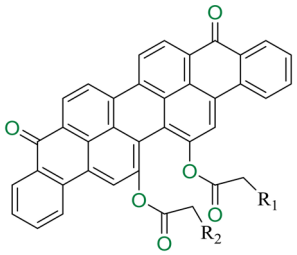

VO-16C: R_1=R_2= $C_{16}H_{33}$
VO-12C: R_1=R_2= $C_{12}H_{25}$
VO-8C: R_1=R_2= C_8H_{17}
VO-4C: R_1=R_2= C_4H_9

Figure 1. Chemical structures of the PA molecular models employed in this work.

Two sets of simulations were performed: (I) in which the 24 solute molecules were of a single type (VO-4C) and (II) where the solutes were a mixture of four types of molecules, containing six molecules of each model. In each case, toluene (a good solvent for the PA compounds),[20] *n*-heptane (a poor solvent for the PA compounds),[21] and heptol (a mixture of *n*-heptane and toluene) of different *n*-heptane/toluene ratios were chosen as the solvents. A total of 16 systems were simulated in this work, and their information is summarized in Table 1. Details of the simulated systems and the explanations on their designations are given below.

2.1. Systems Simulated. The first five systems shown in Table 1 involve only VO-4C as the solute. For each system, 24 VO-4C molecules were initially packed into a cubic box of dimensions 12 × 12 × 12 nm^3, forming a 2 × 3 × 4 array with their PA cores parallel to one another (see Figure 2a). These molecules were then solvated in different solvents: pure toluene in VO-4C-T, heptol with 25% *n*-heptane in VO-4C-HT25, heptol with 50% *n*-heptane in VO-4C-HT50, heptol with 75% *n*-heptane in VO-4C-HT75, and pure *n*-heptane in VO-4C-H.

A similar method was used to build the systems involving a mixture of solutes. Particularly, for system Mixture-T, six molecules of each type of solute (VO-16C, VO-12C, VO-8C, or VO-4C) were arranged to form a 2 × 3 array in the $x-y$ plane (see Figure 2b), where VO-16C is colored purple, VO-12C pink, VO-8C cyan, and VO-4C green. These arrays were then aligned in the z-direction to form a 2 × 3 × 4 matrix, followed by solvation in pure toluene. The mixture was also simulated in pure *n*-heptane (system Mixture-H) and in heptols at seven *n*-heptane/toluene ratios: 12.5:87.5 (system Mixture-HT12.5), 25:75 (system Mixture-HT25), 37.5:62.5 (system Mixture-HT37.5), 50:50 (system Mixture-HT50), 62.5:37.5 (system Mixture-HT62.5), 75:25 (system Mixture-HT75), and 87.5:12.5 (system Mixture-HT87.5).

For each of the system described above, standard MD simulations were performed (details given in section 2.2). As will be demonstrated later, at the late stage of the standard MD simulations, while in system VO-4C-T only short-range stacking was observed, a nearly 1D structure of long-range PA core stacking was formed by the mixture in toluene (system Mixture-T). To make sure such difference was not due to the

DOI: 10.1021/acs.jpcb.5b04481
J. Phys. Chem. B 2015, 119, 8660−8668

Table 1. Information on the 16 Different Systems Simulated[a]

system names	no. of VO molecules	no. of toluene molecules	no. of *n*-heptane molecules	concn of solutes (g/L)	simulation time (ns)
VO-4C-T[20]	24	8857	0	15.8	80
VO-4C-HT25	24	7068	1684	15.8	200
VO-4C-HT50	24	4736	3365	15.8	200
VO-4C-HT75	24	2362	5053	15.8	200
VO-4C−H[21]	24	0	6233	15.8	180
VO-4C-TR	24	8857	0	15.8	220
Mixture-T	24	8751	0	19.7	200
Mixture-HT12.5	24	8126	834	19.7	200
Mixture-HT25	24	6999	1661	19.7	200
Mixture-HT37.5	24	5405	2370	19.7	200
Mixture-HT50	24	4671	3329	19.7	200
Mixture-HT62.5	24	3294	3825	19.7	200
Mixutre-HT75	24	2335	4990	19.7	200
Mixture-HT87.5	24	1163	5278	19.7	200
Mixture-H	24	0	6157	19.7	200
Mixture-TR	24	8751	0	19.7	220

[a]The concentrations of solutes are calculated using the initial size of the simulation box.

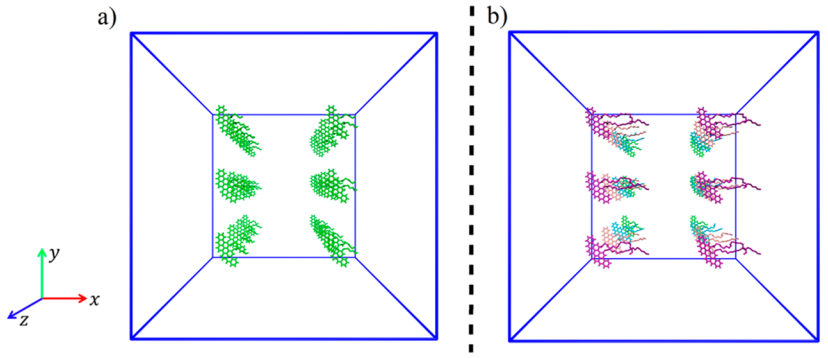

Figure 2. Initial solute configurations: (a) for systems VO-4C-T, VO-4C-HT25, VO-4C-HT50, VO-4C-HT75, and VO-4C−H; (b) for systems Mixture-T, Mixture-HT12.5, Mixture-HT25, Mixture-HT37.5, Mixture-HT50, Mixture-HT62.5, Mixture-HT75, Mixture-HT87.5, and Mixture-H, where different types of VO compounds are represented by different colors.

systems being trapped in potential energy wells, we enhanced the sampling by performing additional replica-exchange MD (REMD) simulations in toluene (systems VO-4C-TR and Mixture-TR in Table 1). The starting configurations for these two systems were adopted from the final structures formed in systems VO-4C-T and Mixture-T.

2.2. Simulation Details. The topologies for VO molecules, toluene and *n*-heptane, which were developed based on GROMOS96 force field parameter set 53A6,[39] were validated in our previous work[20,21,40] and directly adopted here. Detailed information on the development of heptol solvent is available in the Supporting Information (section S1).

Both standard MD and REMD simulations were performed using the MD package GROMACS (version 4.0.7).[41−44] Periodic boundary conditions, full electrostatics with particle-mesh Ewald method,[45] cutoff distance 1.4 nm for van der Waals interactions and electrostatics pairwise calculations, LINCS algorithm to constraint all bonds,[46] and a time step of 2 fs were used in all simulations.

During each standard MD simulation, static structure optimization was first performed to minimize the total potential energy. Then the non-hydrogen atoms of the solutes were restrained with 1000 kJ/(mol nm^2) harmonic potential for 1 ns at 300 K and 1 bar to relax the solvents around the solutes. The restraint was then removed, and NPT ensemble simulation was performed for 80 ns for system VO-4C-T, 180 ns for system VO-4C-H, and 200 ns for the other systems.

REMD is an enhanced sampling technique by simulating copies (replicas) of the same systems to sample conformations at different temperatures and attempting exchanges between neighboring replicas at a certain frequency.[47] By doing so, it helps with overcoming energy barrier on the potential energy surface, thus allowing the exploration of new conformational space. In this work, each run of the two REMD systems, VO-4C-TR and Mixture-TR in Table 1, is composed of 11 replicas at 300, 301.25, 302.5, 303.75, 305, 306.25, 307.5, 308.75, 310, 311.25, and 312.5 K. The temperature distribution was chosen such that an acceptance ratio of 21%−23% was achieved between all replicas. Each replica was run for 20 ns, resulting in a total of 220 ns integration time and 22 000 configurations for each system. Performance of each REMD system was checked using a probability distribution of total potential energy of each replica, and this information is available in the Supporting Information (section S2).

2.3. Data Analysis. Appropriate postprocessing tools available in GROMACS were used for trajectory analysis and VMD[48] used for visualization.

To quantitatively describe the geometry of molecular aggregates in the standard MD simulations, a dimension map method proposed in our recent work[40] was adopted here.

DOI: 10.1021/acs.jpcb.5b04481
J. Phys. Chem. B 2015, 119, 8660−8668

Specifically, using heavy atoms in the PA cores of the molecules in an aggregate, three principal radii of gyration can be calculated and are denoted by R_x, R_y, and R_z. A pair of gyradius ratios (r_1 and r_2) were then defined as

$$r_1 = \frac{R_1}{R_0}, \quad r_2 = \frac{R_2}{R_0} \tag{1}$$

where R_0 is the minimum of $\{R_x, R_y, R_z\}$, R_2 is the maximum of $\{R_x, R_y, R_z\}$, and R_1 is the intermediate value. For a 1D structure, as the length scale in one direction is much larger than that in the other two, $r_2 \approx r_1 \gg 1$. For a sphere-like structure, because the three dimensions are approximately equal, $r_2 \approx r_1 \approx 1$. For a short-cylinder-like structure, the length of the cylinder is comparable to its diameter; thus $r_2 \approx r_1 > 1$. Therefore, gyradius ratios are a good indicator for the dimension characteristics of molecular aggregates, and examining the locations of the points on the dimension map provides an effective way to directly compare the geometries of molecular aggregates.

To evaluate the relative stability of the conformations formed in REMD, we calculated the free energy (potential of mean force) difference ΔW as a function of two reaction coordinates, number of aggregates (n), and size of the largest aggregate (s). Here, the size is defined as the number of molecules inside the largest aggregate. By counting the relative probability of the configurations with different n and s, ΔW is calculated using[49,50]

$$\Delta W(n, s) = -kT \ln \frac{P(n, s)}{P_{max}} = -kT \ln \frac{N(n, s)}{N_{max}} \tag{2}$$

In eq 2, $P(n,s)$ is the probability density obtained from the REMD data, P_{max} is the maximum of $P(n,s)$, $N(n,s)$ is the number of configurations with the same n and s, and N_{max} is the largest of $N(n,s)$. Therefore, the ratio represents the relative probability, and by this definition $\Delta W(n,s) \geq 0$.

3. RESULTS AND DISCUSSION

3.1. Aggregation in Pure Toluene. Figure 3 shows the largest stable aggregates formed in systems VO-4C-T and Mixture-T at the equilibrium stage of the simulations, where different types of VO molecules are represented by different colors. Here, the largest stable aggregates are the ones that do not dissociate at the equilibrium stage of the simulations (the last 10 ns for VO-4C-T and the last 20 ns for Mixture-T). It can be seen from Figure 3 that, irrespective of the solute kinds, the aggregates are mainly formed by the parallel stacking of multiple PA cores, demonstrating the dominant role of $\pi-\pi$ interaction.[19−21,51] In addition, for each of the two aggregates, there exists a clear axis, depicted as blue lines in Figure 3 for a guide to the eye, along which the stacking of PA cores is propagated. However, the parallel stacking formed by mixtures persists for a much longer distance. To be specific, in system VO-4C-T, the largest stable aggregate involves seven molecules and resembles a short cylinder. Such structure is consistent with the well-known Yen−Mullins model[52−54] for asphaltene aggregation in toluene. On the contrary, in system Mixture-T, the largest stable assembly contains 15 molecules, leading to a 1D rod-like structure.

To quantitatively describe these geometry differences, we calculated the gyradius ratios of the PA core regions for the two aggregates shown in Figure 3 using the method described in section 2.3. The corresponding values are respectively $\{r_1 = 1.61, r_2 = 1.73\}$ for VO-4C-T and $\{r_1 = 2.67, r_2 = 2.72\}$ for Mixture-T. These gyradius ratios apparently deviate from the case of $\{r_1 \approx 1, r_2 \approx 1\}$ which are the characteristics of a sphere-like structure. This is consistent with the ordered parallel stacking of PA cores observed. More importantly, the gyradius ratios of the aggregates formed in Mixture-T are much larger than those in VO-4C-T, quantitatively confirming that the parallel stacking is significantly enhanced by having a mixture of solute molecules.

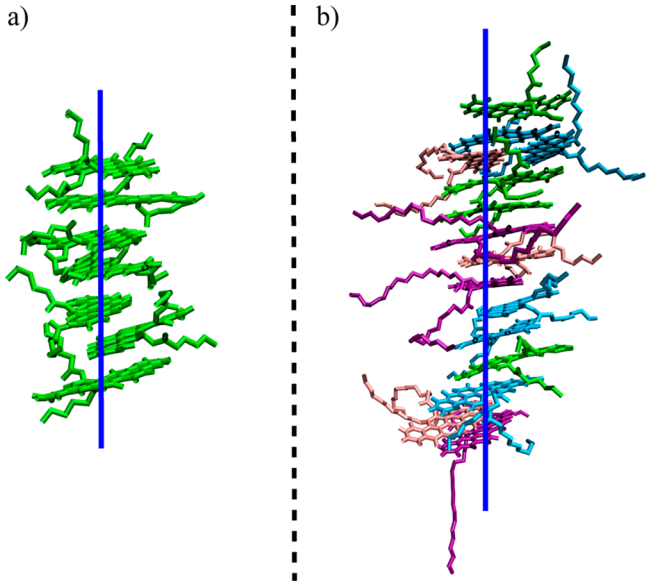

Figure 3. Snapshots of the largest stable aggregates formed at the equilibrium stage of the simulations in systems: (a) VO-4C-T and (b) Mixture-T.

One could argue that the above difference in configuration may be caused by poor sampling in standard MD techniques where the VO molecules are trapped in a potential energy well. To address this, REMD techniques were employed to enhance the configuration sampling of VO-4C and mixtures. Using the method described in section 2.2, in Figure 4, we reported the free energy landscape of aggregation for systems VO-4C-TR and Mixture-TR at 300 K as a function of two reaction coordinates, number of molecular aggregates (n), and size of

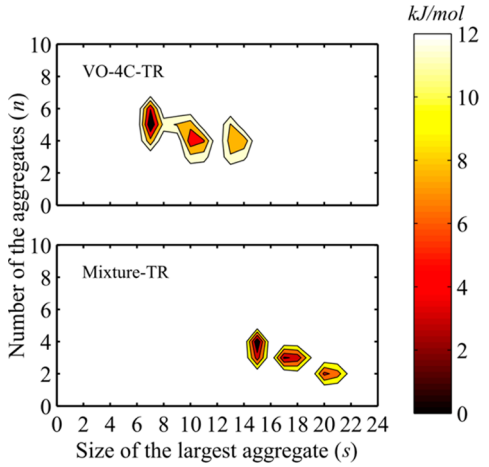

Figure 4. Free energy landscape versus number of the aggregates (n) and size of the largest aggregate (s) for systems VO-4C-TR and Mixture-TR.

DOI: 10.1021/acs.jpcb.5b04481
J. Phys. Chem. B 2015, 119, 8660−8668

the largest aggregate (s). If none of the VO molecules aggregate, the maximum possible value for n is 24. However, in both plots, n is limited to 10, as no data were found for n = 10−24. Figure 4 shows that for system VO-4C-TR the free energy minimum is located at $n \approx 4-6$ and $s \approx 7$, whereas for system Mixture-TR, the most evident free energy minimum is located at $n \approx 3-4$ and $s \approx 15$. It clearly demonstrates that mixture tends to form larger aggregates, resulting in less number of molecular aggregates. As the free energy minimum represents the most probable configuration at a specific temperature, these results confirms previous results from standard MD simulations. To understand the physical meaning behind this interesting phenomenon, below we will take a detailed look at the aggregated structures.

Further inspection of Figure 3b shows that molecules of different types, denoted by different colors, appear in an alternating manner. If we "sequence" the aggregate from top to bottom, then the four types of molecules appear in the following order (omitting "VO" for simplicity): 4C-8C-8C(12C)-4C-4C-16C-12C-16C-8C-8C-4C-8C-12C-16C, where 8C(12C) denotes the one VO-8C molecule and one VO-12C molecule that are located in a side-by-side manner. It seems that $\pi-\pi$ stacking in the aggregate is more likely to be formed between molecules of different types. To quantify the $\pi-\pi$ interaction among these PA molecules, we first introduced the molecule identification (ID) number and labeled the molecules in system Mixture-T by numbers 1−24. Specifically, numbers 1−6 were used to label the 6 VO-4C molecules, followed by number 7−12 for VO-8C molecules, 13−18 for VO-12C molecules, and 19−24 for VO-16C molecules. Then for each pair of PA cores, the minimum distance between their PA cores was calculated every 100 ps, resulting in 2000 data points during the 200 ns simulation run. A $\pi-\pi$ contact is counted if this minimum distance is $\leq$0.5 nm.[9,55] If out of the 2000 data points the total number of $\pi-\pi$ contacts is $\geq$1000 over the whole simulation course, i.e., the two PA cores are in $\pi-\pi$ contact for at least 50% of the simulation time, then we say the two PA cores are stably stacked. Figure 5 shows the pairwise stacking table, where the x- and y-axes represent the molecule ID number and a grid point will be marked with a blue square if a stable stacked pair is formed between molecules x and y. Because of symmetry, only the upper left half of the grid is utilized. Stacking that falls in the purple triangular region are the ones formed between the VO molecules of the same type. It can be clearly seen that, in total, six stacking pairs are formed between VO molecules of the same type. On the other hand, there are 12 pairs outside the purple triangular regions, which demonstrates that the $\pi-\pi$ stacking is more likely to be formed between molecules of different types, consistent with previous observation in Figure 3b. As it has been reported[20] that for a single type of PA molecules only short-ranged stacking was found in pure toluene, the results shown here suggest that the alternating stacking manner of PA mixtures can introduce advantages to increasing the stacking range. These advantages are analyzed in detail below.

In toluene, longer side chains have been proposed to reduce the flexibility of PA molecules and provide larger steric hindrance to $\pi-\pi$ stacking, thus limiting the stacking range.[20] For instance, in our previous work,[20] it has been shown that long side chains prohibits the formation of large direct parallel stacking structures that involve more than three molecules. When multiple types of VO compounds coaggregate, short-chained molecules can exist between long-chained ones. By having smaller molecules in between, the steric hindrance of long side chains were decreased. This is the first advantage the mixture brings to promoting long-range stacking.

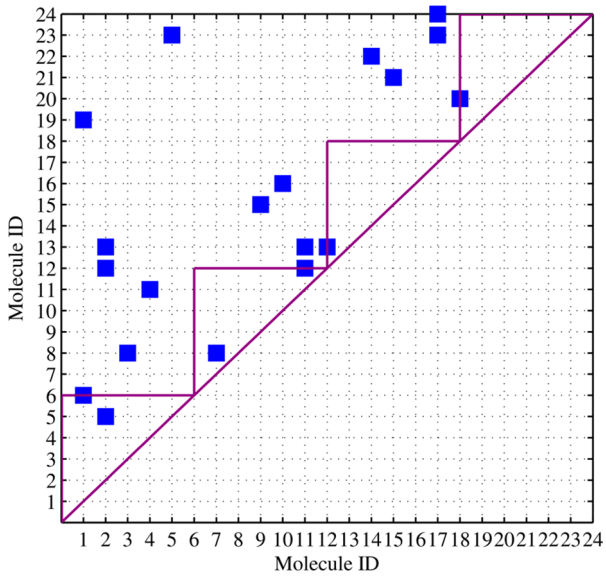

Figure 5. Pairwise stacking table for system Mixture-T. The x- and y-axes represent the molecule ID number (1 to 24, representing the 24 molecules in the simulation system), and the grid point marked with a blue square indicates that a stable stacked pair is formed between molecules x and y. Symbols in the purple triangular region correspond to the stable stacking formed between the VO molecules of the same type. Because of symmetry, only the upper left half of the grid is utilized.

The second advantage lies in the "protection" long-chained molecules bring to the short-chained molecules. It has been proved[20] that toluene is a good solvent for the PA molecules because they can have attractive interactions with the PA cores. When short-chained molecules stack, toluene molecules can diffuse into the space between neighboring molecules and break the $\pi-\pi$ stacking through their attraction with the PA cores. However, if these PA molecules with short side chains are sandwiched between molecules with longer side chains, the PA cores are better "protected" and the solvent−solute attractions are reduced, thus helping with stacking. To clearly show the protection from the long side chains, we performed three additional simulations, each of which has three VO molecules forming parallel stacking in toluene. Specifically, two systems involve three VO molecules of a single type (VO-4C or VO-16C) and will be respectively referred to as systems 4C-4C-4C and 16C-16C-16C. The third system, referred to as 16C-4C-16C, contains a mixture of VO-4C and VO-16C types of molecules, where the parallel stacked structure is of the "sequence" 16C-4C-16C. Thus, comparison for the toluene distribution around the PA core in the three systems can provide direct information about the "protection" roles of long-chained molecules. Figure 6 shows the radial distribution function (RDF) and the cumulative number (CN) of toluene atoms around the atoms on the PA core of the middle molecule (e.g., 4C in 16C-4C-16C). It can be seen that in the RDF and CN plots the curve for system 16C-4C-16C nearly overlaps with the one for system 16C-16C-16C and is below the one for system 4C-4C-4C. The smaller values of RDF and CN here confirm that at a given distance there is less contact, hence less attraction, between toluene molecules and the VO molecule in

DOI: 10.1021/acs.jpcb.5b04481
J. Phys. Chem. B 2015, 119, 8660−8668

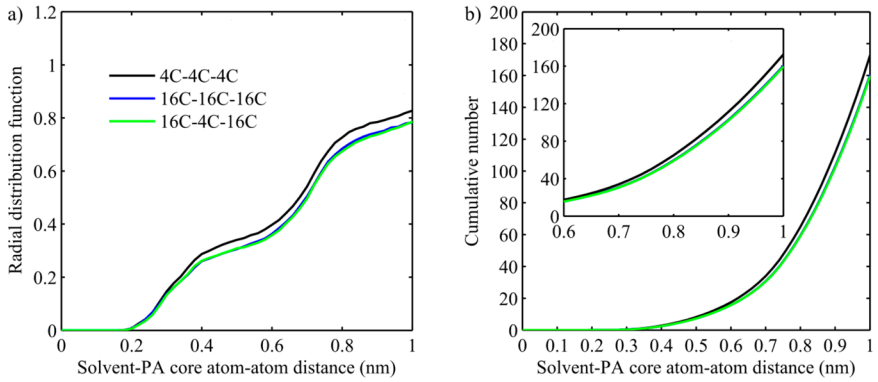

Figure 6. (a) RDF and (b) CN for the distance between toluene atoms and PA core atoms (middle molecule). The inset in (b) shows the enlarged CN for atom−atom distance from 0.6 to 1 nm.

the middle of the stacking in systems 16C-4C-16C and 16C-16C-16C.

3.2. Aggregation in Heptol. It has been shown in the previous section that in pure toluene the stacking range and formation of 1D rod-like structure have been enhanced by having a mixture of VO molecules as solutes. As the property of the solvent is a crucial factor that can influence the structure of the aggregates,[11] it is of great interest to investigate the variation of aggregated structures with the change of solvents. It was shown in our previous work[20,21] that for a single type of PA molecules, while the stacked PA cores resemble short cylinders in toluene, a 1D rod-like structure of long-range stacked PA cores was formed in *n*-heptane. The enhanced aggregation/association of PA compounds in *n*-heptane, compared with that in toluene, has also been reported in the work of Headen et al.[56] and Sedghi et al.[57] Therefore, we chose to vary the solvent from pure toluene to pure *n*-heptane by increasing the *n*-heptane ratio, and the results are shown below.

Figure 7 shows the dimension map generated using the PA core region of the aggregated structures formed by VO-4C in toluene, heptol (three different heptol ratios), and *n*-heptane. The corresponding dimension map for the aggregates formed by the mixture of solutes is given by Figure 8, with four

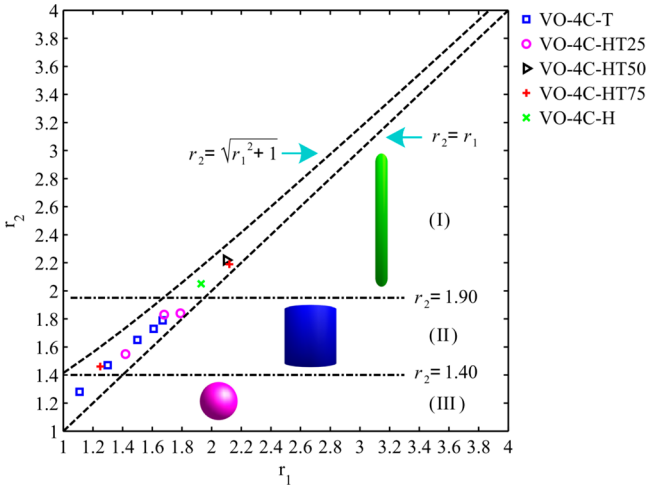

Figure 7. Dimension map for systems with VO-4C as solutes. Different symbols correspond to simulations with different solvents. There may be more than one aggregate in a particular system, and each aggregate is represented by a separate point. Each of the three regimes I, II, and III corresponds to a particular group of structures: regime I represents 1D rod-like structures, regime II represents short-cylinder-like structures, and regime III represents three-dimensional sphere-like structures.

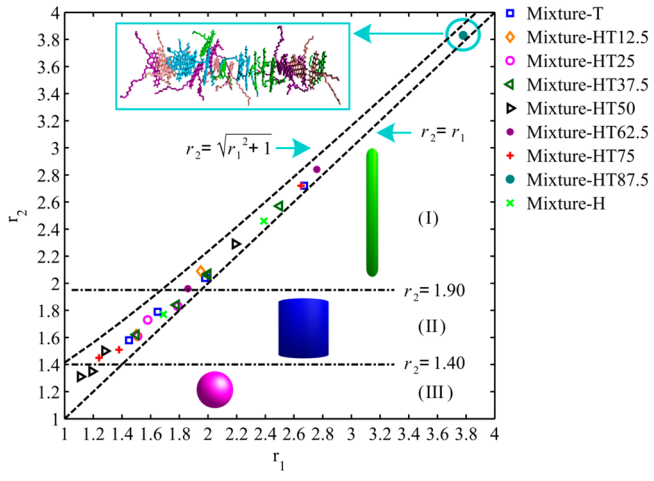

Figure 8. Dimension map for systems with a mixture of different VO molecules as solutes. Different symbols correspond to simulations with different solvents. There may be more than one aggregate in a particular system, and each aggregate is represented by a separate point. Each of the three regimes I, II, and III corresponds to a particular group of structures: regime I represents 1D rod-like structures, regime II represents short-cylinder-like structures, and regime III represents three-dimensional sphere-like structures.

additional Heptol ratios. There may be more than one aggregate in each system, and each aggregate is represented by a separate symbol. As proven in our previous work,[40] all the data on the dimension map are bounded by two curves $r_2 = r_1$ and $r_2 = (r_1^2 + 1)^{1/2}$, plotted as black dashed lines. To further investigate the distribution of gyradius ratios, we divided each dimension map into three regimes, each corresponding to a particular group of structures: (I) $r_2 \geq 1.90$, which represents 1D rod-like structures (the stacking range is much larger than the dimensions in the PA core plane); (II) $1.40 < r_2 < 1.90$, which represents short-cylinder-like structures (the stacking range is comparable to the dimensions in the PA core plane); (III) $r_2 \leq 1.40$, which represents three-dimensional sphere-like structures (PA cores entangled together without preferred stacking directions). The boundary lines separating the three regimes were chosen based on the natural gaps found on the dimension map in Figure 7 and applied to Figure 8 as well.

DOI: 10.1021/acs.jpcb.5b04481
J. Phys. Chem. B 2015, 119, 8660−8668

The first observation made from Figures 7 and 8 is that in both figures almost all of the data are located above r_2 = 1.4, below which aggregates of sphere-like shapes locate. This is consistent with the ordered structures visually observed earlier. Despite these similarities, detailed examination reveals that considerable differences can be found between the two dimension maps. Let us first consider Figure 7. Clearly, the gyradius ratios for the aggregates formed in system VO-4C-T, depicted as blue squares, are mainly located in regime II, indicating that the aggregated PA cores are of short-range stacking. As *n*-heptane ratio increases in the solvent, the parallel stacking of PA cores is enhanced, and consequently the gyradius ratios show a trend of moving into regime I. At sufficiently high *n*-heptane/toluene ratios (>25%), the gyradius ratios mostly lie in regime I and are well distinguished from those of system VO-4C-T, corresponding to the long-range stacking of PA cores. On the contrary, in Figure 8, aggregates in regime I are present for all types of solvents except when *n*-heptane/toluene ratio = 25%:75%. That is, given a mixture as the solutes, the existence of 1D rod-like structure becomes insensitive to the type of solvent. Second, at the same *n*-heptane/toluene ratios, the largest gyradius ratio from a system involving mixtures is generally larger than its counterpart with VO-4C as the solute. For instance, at 75%:25% (*n*-heptane/toluene ratio), the largest pair of gyradius ratios for system Mixture-HT75 is $\{r_1 \approx 2.6, r_2 \approx 2.7\}$ while the corresponding values for VO-4C-HT75 are $\{r_1 \approx 2.1, r_2 \approx 2.2\}$. Finally, a nearly straight 1D structure with infinity curvature (hence the largest gyradius ratios) is formed in system Mixture-HT87.5, shown as the inset in Figure 8, which is not observed in systems involving solely VO-4C as solute. If we "sequence" this structure (see section S3 in the Supporting Information), again, molecules of different types stack together in an alternating manner. All these observations further support previous conclusion that by having mixtures as solute, parallel stacking of PA cores is enhanced.

One interesting observation, as mentioned above, is that the largest gyradius ratios found in Figure 8 are not formed by mixture in pure *n*-heptane, but rather in heptol with 87.5% *n*-heptane. Examination of Figure 7 also shows that the largest gyradius ratios for VO-4C are found in systems with heptol being the solvents (i.e., systems VO-4C-HT50 and VO-4C-HT75). While intuitively adding *n*-heptane should help with PA core stacking, the observation here seems to indicate that this effect is not monotonic. In other words, the longest range of stacking is achieved when a small amount of toluene is present. To understand this, it is necessary to take a detailed look at the aggregation mechanism.

It has been proved[20,21] that, compared with *n*-heptane, toluene can form $\pi-\pi$ stacking with PA molecules, which reduces the interaction between PA cores ($\pi-\pi$ interaction), between PA core and side chain ($\pi-\theta$ interaction), and between side chains ($\theta-\theta$ interaction). Among these three types of solute−solute interactions, $\pi-\pi$ interaction is the main force driving the formation of 1D rod-like structure, while $\pi-\theta$ and $\theta-\theta$ interactions bring in adverse effect that interfere with the parallel stacking of PA cores. With the increase of the *n*-heptane ratio in the solvents, all three types of interactions are increased (see evidence using intermolecular contacts; details given in the Supporting Information, section S4), thus resulting in a larger aggregate. On the other hand, when the *n*-heptane ratio is too high, for instance, in the case of pure *n*-heptane, the large amount of $\pi-\theta$ and $\theta-\theta$ interactions can introduce relative titling, slipping, and twisting between neighboring PA cores. This reduces the likelihood of forming "perfect parallel stacking" where one PA core is parallel to another with the line connecting their centers perpendicular to the PA planes.[21] Therefore, to maximize the stacking range in the 1D structure, the optimum solvent should simultaneously promote the $\pi-\pi$ interaction between solutes and avoid too much increase in the $\pi-\theta$ and $\theta-\theta$ interactions. This explains why the largest gyradius ratios in Figures 7 and 8 are from systems with heptol as solvents instead of pure *n*-heptane.

3.3. Implications. Obtaining 1D structure of parallel-stacked PA cores is of crucial importance in the design of optical and electrical nanodevices.[1,3] For the PA compounds studied here, the present work provides two potential methods that can be employed in practice. First, for a given solute, the stacking of PA cores can be enhanced through selecting appropriate solvents. The optimal solvent is the one that can increase the $\pi-\pi$ interaction between PA cores without introducing too much association between side chains and between side chains and PA cores.

Second and also more importantly, for a given solvent, the stacking of PA cores can be enhanced by introducing inhomogeneity into the solutes. To obtain a 1D structure in a given solvent, a typical approach in the literature is to synthesize new-functionalized PA molecules.[1,21−24] However, instead of looking for a new kind of solutes, our results suggest that simply mixing different types of PA molecules in hand may provide an additional approach to generate 1D structure, thus avoiding the design of new synthetic procedure. Furthermore, as shown earlier, for a mixture of solutes the existence of the 1D aggregates is not so sensitive to the solvents, although the composition of the solvent can affect the degrees of stacking inside the 1D structure. Therefore, having a solute mixture may allow more flexibility in choosing appropriate solvents.

Finally, it is of great importance to point out that although a particular type of PA compounds is studied here, these molecules possess the common features of PA compounds. Therefore, the results discussed in this work can be applied to a broader class. For instance, to precipitate industrial PA compounds, such as asphaltenes, precipitants ("bad" solvents) are usually added to heavy oil solutions.[58] The aggregation behaviors in heptol investigated here can provide information about the amount of precipitants needed for effective precipitation.

4. CONCLUSIONS

In this work, we investigated the effect of inhomogeneity in solute on the aggregation of our representative PA compounds using all-atom MD simulations. The PA compounds studied here are differentiated by their side-chain lengths. In toluene, we found that compared with a single type of PA compound, parallel stacking of PA cores were enhanced by having a mixture of four types of PA compounds. Specifically, PA compounds of different types organize themselves in an alternating manner. This alternating stacking manner reduces the steric hindrance of long side chains and shields the attractive interaction between toluene molecules and the PA cores, allowing the assembly of a 1D rod-like structure with long-range stacking. It was further shown that while for a single type of PA compound the 1D rod-like structure could only be formed in pure *n*-heptane or heptol of sufficiently large *n*-heptane/toluene ratio, the existence of the 1D structure formed by mixtures is insensitive to the composition of the solvents.

DOI: 10.1021/acs.jpcb.5b04481
J. Phys. Chem. B 2015, 119, 8660−8668

However, solvents can tune the stacking manner of PA cores by affecting the intermolecular interactions among the solutes. To achieve "perfect" stacking, the solvent should simultaneously increase the interaction between PA cores and avoid introducing too much association between PA core and side chain as well as between side chains. These results shed light on how one may control the aggregation of PA compounds by adjusting solute as well as solvent.

■ ASSOCIATED CONTENT

Supporting Information

Development of heptol solvent; probability distribution of total potential energy in the replica-exchange molecular dynamics (REMD) simulations; structural "sequence" of the aggregate formed in system Mixture-HT87.5; intermolecular contacts formed between PA compounds. The Supporting Information is available free of charge on the ACS Publications website at DOI: 10.1021/acs.jpcb.5b04481.

■ AUTHOR INFORMATION

Corresponding Author

*Phone +1-780-492-5467; Fax +1-780-492-2200; e-mail tian.tang@ualberta.ca (T.T.).

Notes

The authors declare no competing financial interest.

■ ACKNOWLEDGMENTS

We acknowledge the computing resources and technical support from Western Canada Research Grid (WestGrid). Financial support for this research from Canada Foundation for Innovation and Alberta Innovates-Technology Futures (AI-TF) is gratefully acknowledged. Cuiying Jian acknowledges financial support from University of Alberta Doctoral Recruitment Scholarship, the Jacob H Masliyah Graduate Award in Oil Sands Engineering, and Alberta Innovates Graduate Student Scholarship.

■ REFERENCES

(1) Zang, L.; Che, Y.; Moore, J. S. One-Dimensional Self-Assembly of Planar π-Conjugated Molecules: Adaptable Building Blocks for Organic Nanodevices. *Acc. Chem. Res.* **2008**, *41*, 1596−1608.

(2) Groenzin, H.; Mullins, O. C. Asphaltene Molecular Size and Structure. *J. Phys. Chem. A* **1999**, *103*, 11237−11245.

(3) Kim, F. S.; Ren, G.; Jenekhe, S. A. One-Dimensional Nanostructures of π-Conjugated Molecular Systems: Assembly, Properties, and Applications from Photovoltaics, Sensors, and Nanophotonics to Nanoelectronics. *Chem. Mater.* **2010**, *23*, 682−732.

(4) Speight, J. Petroleum Asphaltenes-Part 1: Asphaltenes, Resins and the Structure of Petroleum. *Oil Gas Sci. Technol.* **2004**, *59*, 467−477.

(5) Spiecker, P. M.; Gawrys, K. L.; Trail, C. B.; Kilpatrick, P. K. Effects of Petroleum Resins on Asphaltene Aggregation and Water-in-Oil Emulsion Formation. *Colloids Surf., A* **2003**, *220*, 9−27.

(6) Kilpatrick, P. K. Water-in-Crude Oil Emulsion Stabilization: Review and Unanswered Questions. *Energy Fuels* **2012**, *26*, 4017−4026.

(7) Bai, S.; Debnath, S.; Javid, N.; Frederix, P. W.; Fleming, S.; Pappas, C.; Ulijn, R. V. Differential Self-Assembly and Tunable Emission of Aromatic Peptide Bola-Amphiphiles Containing Perylene Bisimide in Polar Solvents Including Water. *Langmuir* **2014**, *30*, 7576−7584.

(8) Su, W.; Zhang, Y.; Zhao, C.; Li, X.; Jiang, J. Self-Assembled Organic Nanostructures: Effect of Substituents on the Morphology. *ChemPhysChem* **2007**, *8*, 1857−1862.

(9) Pisula, W.; Feng, X.; Müllen, K. Tuning the Columnar Organization of Discotic Polycyclic Aromatic Hydrocarbons. *Adv. Mater.* **2010**, *22*, 3634−3649.

(10) Safont-Sempere, M. M.; Fernández, G.; Würthner, F. Self-Sorting Phenomena in Complex Supramolecular Systems. *Chem. Rev.* **2011**, *111*, 5784−5814.

(11) Yoosuf Ameen, M.; Abhijith, T.; De, S.; Ray, S.; Reddy, V. Linearly Polarized Emission from PTCDI-C_8 One-Dimensional Microstructures. *Org. Electron.* **2013**, *14*, 554−559.

(12) Islam, M. R.; Sundararajan, P. Self-Assembly of a Set of Hydrophilic−Solvophobic Hydrophobic Coil−Rod−Coil Molecules Based on Perylene Diimide. *Phys. Chem. Chem. Phys.* **2013**, *15*, 21058−21069.

(13) Jang, K.; Kinyanjui, J. M.; Hatchett, D. W.; Lee, D. Morphological Control of One Dimensional Nanostructures of T-Shaped Asymmetric Bisphenazine. *Chem. Mater.* **2009**, *21*, 2070−2076.

(14) Wu, H.; Xue, L.; Shi, Y.; Chen, Y.; Li, X. Organogels Based on J- and H-Type Aggregates of Amphiphilic Perylenetetracarboxylic Diimides. *Langmuir* **2011**, *27*, 3074−3082.

(15) Verdier, S.; Carrier, H.; Andersen, S. I.; Daridon, J. Study of Pressure and Temperature Effects on Asphaltene Stability in Presence of CO_2. *Energy Fuels* **2006**, *20*, 1584−1590.

(16) Wang, C.; Dong, H.; Hu, W.; Liu, Y.; Zhu, D. Semiconducting π-Conjugated Systems in Field-Effect Transistors: A Material Odyssey of Organic Electronics. *Chem. Rev.* **2011**, *112*, 2208−2267.

(17) Figueira-Duarte, T. M.; Müllen, K. Pyrene-Based Materials for Organic Electronics. *Chem. Rev.* **2011**, *111*, 7260−7314.

(18) Kuznicki, T.; Masliyah, J. H.; Bhattacharjee, S. Molecular Dynamics Study of Model Molecules Resembling Asphaltene-Like Structures in Aqueous Organic Solvent Systems. *Energy Fuels* **2008**, *22*, 2379−2389.

(19) Jian, C.; Tang, T.; Bhattacharjee, S. Probing the Effect of Side Chain Length on the Aggregation of a Model Asphaltene Using Molecular Dynamics Simulations. *Energy Fuels* **2013**, *27*, 2057−2067.

(20) Jian, C.; Tang, T.; Bhattacharjee, S. Molecular Dynamics Investigation on the Aggregation of Violanthrone78-based Model Asphaltenes in Toluene. *Energy Fuels* **2014**, *28*, 3604−3613.

(21) Jian, C.; Tang, T. One-dimensional Self-assembly of Poly-aromatic Compounds Revealed by Molecular Dynamics Simulations. *J. Phys. Chem. B* **2014**, *118*, 12772−12780.

(22) Balakrishnan, K.; Datar, A.; Oitker, R.; Chen, H.; Zuo, J.; Zang, L. Nanobelt Self-Assembly from an Organic n-Type Semiconductor: Propoxyethyl-PTCDI. *J. Am. Chem. Soc.* **2005**, *127*, 10496−10497.

(23) Balakrishnan, K.; Datar, A.; Naddo, T.; Huang, J.; Oitker, R.; Yen, M.; Zhao, J.; Zang, L. Effect of Side-Chain Substituents on Self-Assembly of Perylene Diimide Molecules: Morphology Control. *J. Am. Chem. Soc.* **2006**, *128*, 7390−7398.

(24) Datar, A.; Balakrishnan, K.; Zang, L. One-Dimensional Self-Assembly of a Water Soluble Perylene Diimide Molecule by pH Triggered Hydrogelation. *Chem. Commun.* **2013**, *49*, 6894−6896.

(25) Che, Y.; Datar, A.; Balakrishnan, K.; Zang, L. Ultralong Nanobelts Self-Assembled from an Asymmetric Perylene Tetracarboxylic Diimide. *J. Am. Chem. Soc.* **2007**, *129*, 7234−7235.

(26) Klein, G. C.; Kim, S.; Rodgers, R. P.; Marshall, A. G.; Yen, A.; Asomaning, S. Mass Spectral Analysis of Asphaltenes. I. Compositional Differences between Pressure-Drop and Solvent-Drop Asphaltenes Determined by Electrospray Ionization Fourier Transform Ion Cyclotron Resonance Mass Spectrometry. *Energy Fuels* **2006**, *20*, 1965−1972.

(27) Klein, G. C.; Kim, S.; Rodgers, R. P.; Marshall, A. G.; Yen, A. Mass Spectral Analysis of Asphaltenes. II. Detailed Compositional Comparison of Asphaltenes Deposit to Its Crude Oil Counterpart for Two Geographically Different Crude Oils by ESI FT-ICR MS. *Energy Fuels* **2006**, *20*, 1973−1979.

(28) Ryan, D. M.; Doran, T. M.; Nilsson, B. L. Complementary π−π Interactions Induce Multicomponent Coassembly into Functional Fibrils. *Langmuir* **2011**, *27*, 11145−11156.

DOI: 10.1021/acs.jpcb.5b04481
J. Phys. Chem. B 2015, 119, 8660−8668

(29) Sakai, H.; Watanabe, K.; Asanomi, Y.; Kobayashi, Y.; Chuman, Y.; Shi, L.; Masuda, T.; Wyttenbach, T.; Bowers, M. T.; Uosaki, K. Formation of Functionalized Nanowires by Control of Self-Assembly Using Multiple Modified Amyloid Peptides. *Adv. Funct. Mater.* **2013**, *23*, 4881−4887.
(30) Bu, L.; Pentzer, E.; Bokel, F. A.; Emrick, T.; Hayward, R. C. Growth of Polythiophene/Perylene Tetracarboxydiimide Donor/Acceptor Shish-Kebab Nanostructures by Coupled Crystal Modification. *ACS Nano* **2012**, *6*, 10924−10929.
(31) Bu, L.; Dawson, T. J.; Hayward, R. C. Tailoring Ultrasound-Induced Growth of Perylene Diimide Nanowire Crystals from Solution by Modification with Poly(3-hexylthiophene). *ACS Nano* **2015**, *9*, 1878−1885.
(32) Zhang, S.; Sun, L. L.; Xu, J.; Wu, H.; Wen, H. Aggregate Structure in Heavy Crude Oil: Using a Dissipative Particle Dynamics Based Mesoscale Platform. *Energy Fuels* **2010**, *24*, 4312−4326.
(33) Zhang, S.; Xu, J.; Wen, H.; Bhattacharjee, S. Integration of Rotational Algorithms into Dissipative Particle Dynamics: Modeling Polyaromatic Hydrocarbons on the Meso-Scale. *Mol. Phys.* **2011**, *109*, 1873−1888.
(34) Zhang, L.; Greenfield, M. L. Molecular Orientation in Model Asphalts using Molecular Simulation. *Energy Fuels* **2007**, *21*, 1102−1111.
(35) Ortega-Rodriguez, A.; Lira-Galeana, C.; Ruiz-Morales, Y.; Cruz, S. Interaction Energy in Maya-Oil Asphaltenes: A Molecular Mechanics Study. *Petrol. Sci. Technol.* **2001**, *19*, 245−256.
(36) Takanohashi, T.; Sato, S.; Saito, I.; Tanaka, R. Molecular Dynamics Simulation of the Heat- Induced Relaxation of Asphaltene Aggregates. *Energy Fuels* **2003**, *17*, 135−139.
(37) Aguilera-Mercado, B.; Herdes, C.; Murgich, J.; Müller, E. Mesoscopic Simulation of Aggregation of Asphaltene and Resin Molecules in Crude Oils. *Energy Fuels* **2006**, *20*, 327−338.
(38) Ortega-Rodríguez, A.; Cruz, S.; Gil-Villegas, A.; Guevara-Rodriguez, F.; Lira-Galeana, C. Molecular View of the Asphaltene Aggregation Behavior in Asphaltene-Resin Mixtures. *Energy Fuels* **2003**, *17*, 1100−1108.
(39) Oostenbrink, C.; Villa, A.; Mark, A. E.; Van Gunsteren, W. F. A Biomolecular Force Field Based on the Free Enthalpy of Hydration and Solvation: The GROMOS Force-Field Parameter Sets 53A5 and 53A6. *J. Comput. Chem.* **2004**, *25*, 1656−1676.
(40) Jian, C.; Tang, T.; Bhattacharjee, S. A Dimension Map for Molecular Aggregates. *J. Mol. Graphics Modell.* **2015**, *58*, 10−15.
(41) Hess, B.; Kutzner, C.; van der Spoel, D.; Lindahl, E. GROMACS 4: Algorithms for Highly Efficient, Load-Balanced, and Scalable Molecular Simulation. *J. Chem. Theory Comput.* **2008**, *4*, 435−447.
(42) Van Der Spoel, D.; Lindahl, E.; Hess, B.; Groenhof, G.; Mark, A. E.; Berendsen, H. J. GROMACS: Fast, Flexible, and Free. *J. Comput. Chem.* **2005**, *26*, 1701−1718.
(43) Lindahl, E.; Hess, B.; Van Der Spoel, D. GROMACS 3.0: A Package for Molecular Simulation and Trajectory Analysis. *J. Mol. Model.* **2001**, *7*, 306−317.
(44) Berendsen, H. J.; van der Spoel, D.; van Drunen, R. GROMACS: A Message-Passing Parallel Molecular Dynamics Implementation. *Comput. Phys. Commun.* **1995**, *91*, 43−56.
(45) Essmann, U.; Perera, L.; Berkowitz, M. L.; Darden, T.; Lee, H.; Pedersen, L. G. A Smooth Particle Mesh Ewald Method. *J. Chem. Phys.* **1995**, *103*, 8577.
(46) Hess, B. P-LINCS: A Parallel Linear Constraint Solver for Molecular Simulation. *J. Chem. Theory Comput.* **2008**, *4*, 116−122.
(47) Sugita, Y.; Okamoto, Y. Replica-Exchange Molecular Dynamics Method for Protein Folding. *Chem. Phys. Lett.* **1999**, *314*, 141−151.
(48) Humphrey, W.; Dalke, A.; Schulten, K. VMD: Visual Molecular Dynamics. *J. Mol. Graphics* **1996**, *14*, 33−38.
(49) Sugita, Y.; Kitao, A.; Okamoto, Y. Multidimensional Replica-Exchange Method for Free Energy Calculations. *J. Chem. Phys.* **2000**, *113*, 6042−6051.
(50) Yu, T.; Schatz, G. C. Free-Energy Landscape for Peptide Amphiphile Self-Assembly: Stepwise versus Continuous Assembly Mechanisms. *J. Phys. Chem. B* **2013**, *117*, 14059−14064.
(51) Buenrostro-Gonzalez, E.; Groenzin, H.; Lira-Galeana, C.; Mullins, O. C. The Overriding Chemical Principles That Define Asphaltenes. *Energy Fuels* **2001**, *15*, 972−978.
(52) Mullins, O. C.; Sabbah, H.; Eyssautier, J.; Pomerantz, A. E.; Barre, L.; Andrews, A. B.; Ruiz-Morales, Y.; Mostowfi, F.; McFarlane, R.; Goual, L.; et al. Advances in Asphaltene Science and the Yen−Mullins Model. *Energy Fuels* **2012**, *26*, 3986−4003.
(53) Mullins, O. C. The Modified Yen Model. *Energy Fuels* **2010**, *24*, 2179−2207.
(54) Mullins, O. C. The Asphaltenes. *Annu. Rev. Anal. Chem.* **2011**, *4*, 393−418.
(55) Pisula, W.; Tomovic, Z.; Simpson, C.; Kastler, M.; Pakula, T.; Müllen, K. Relationship between Core Size, Side Chain Length, and the Supramolecular Organization of Polycyclic Aromatic Hydrocarbons. *Chem. Mater.* **2005**, *17*, 4296−4303.
(56) Headen, T. F.; Boek, E. S.; Skipper, N. T. Evidence for Asphaltene Nanoaggregation in Toluene and Heptane from Molecular Dynamics Simulations. *Energy Fuels* **2009**, *23*, 1220−1229.
(57) Sedghi, M.; Goual, L.; Welch, W.; Kubelka, J. Effect of Asphaltene Structure on Association and Aggregation Using Molecular Dynamics. *J. Phys. Chem. B* **2013**, *117*, 5765−5776.
(58) Speight, J. G.; Long, R. B.; Trowbridge, T. D. Factors Influencing the Separation of Asphaltenes from Heavy Petroleum Feedstocks. *Fuel* **1984**, *63*, 616−620.

DOI: 10.1021/acs.jpcb.5b04481
J. Phys. Chem. B 2015, 119, 8660−8668